CRYSTALLOGRAPHY REPORTS, 2025, Vol. 70, No. 1, pp. 135–157

CRYSTALLOGRAPHIC METHODS IN HUMANITIES

CHEMICAL COMPOSITION OF POLYCHROME ENAMELS OF THREE ANCIENT RUSSIAN BRONZE ITEMS FROM VLADIMIR-SUZDAL RUSSIA

E. K. Stolyarova[a,*], T. F. Mukhina[b], A. M. Ismagulov[c], P. A. Volkov[c], A. G. Kulikov[c], E. Yu. Tereschenko[c], and E. B. Yatsishina[c]

[a] *Lomonosov Moscow State University, Moscow, Russia*
[b] *Independent researcher, Vladimir, Russia*
[c] *National Research Center "Kurchatov Institute", Moscow, Russia*
**e-mail: kath.stoliarova@gmail.com*

Received September 26, 2024
Revised November 06, 2024
Accepted November 14, 2024

Abstract. The basic composition of polychrome enamels of three bronze items found on the territory of Vladimir and Suzdal Opolje dating from the 12th and 13th centuries (a temporal pendant, a pendant icon and a cross) was studied by atomic emission spectroscopy and energy dispersive X-ray microanalysis. The items have rich coloration, which allowed us to study the technological features of a wide range of colored enamels: white, black, gray, light gray, deep-blue, red-brown, brown, green, blue-green, turquoise, yellow. The obtained results suggested the Byzantine origin of the enamels and the local production of the items themselves.

DOI: 10.31857/S00234761250119e5

INTRODUCTION

Researchers have long been interested in the chemical composition of Byzantine and Old Russian enamels. In Russian historiography, the first author to report this information was N.P. Kondakov [1]. (In an earlier work, I.E. Zabelin also provides recipes for "finift mass", but these pertain to Western production of the 17th–18th centuries [2, P. 21]). Kondakov presents his findings in his work dedicated to Byzantine objects with enamels from the collection of A.V. Zvenigorodsky. At that time, the understanding of enamel composition was limited to components such as lead, which ensured the "purity and vibrancy of enamel colors", and borax (sodium borate, sodium tetraborate, $Na_2B_4O_7$). An exception was considered to be purple enamel, which was believed to be produced without lead. The colorants were thought to include cobalt oxide for blue enamel, copper for green, manganese for lilac, tin for opaque white, and cuprous oxide with iron oxide for red. For purple enamel, N.P. Kondakov suggested the use of Cassius purple – gold precipitated with stannic chloride [1, P. 93–94]. However, this method of coloring glass, now known as "gold ruby", was only discovered in the 17th century [3, P. 50] and was evidently not used for earlier enamels. Overall, the author's views on the composition and colorants of Byzantine enamels were not based on studies of specific enamels but rather on general knowledge of glass from that period.

A new stage in the study of enamel compositions in Russian science began in the 1960s–1970s, when Byzantine and Old Russian enamelled objects started to be examined using scientific methods. In particular, Georgian researchers worked in this field [4, P. 7]. At Moscow University, a study was conducted on an enamel plaque found in Lyubech, which revealed a sodium-lead composition, colored with cobalt and decolorized with manganese. According to the author of the analysis, Yu.L. Shchapova, this indicated a Byzantine origin for the enamel [4, P. 16]. However, the limitations of the research methods available at that time did not allow for the accumulation of a sufficiently large database on enamel compositions. As a result, researchers had to rely on scattered data, which led to the use of information from modern enamel technology, which in some cases did not correspond to ancient techniques. For example, chromium compounds, which are used in contemporary production to create yellow and green enamels, were not used in antiquity, as noted by T.I. Makarova [4, P. 16; 5, P. 45, 46, 48].

The aim of this study is to examine the chemical (elemental) composition of pre-Mongol enamels using modern analytical methods. This information will help address questions of enamel provenance and chronology. At this stage, it is sufficient to consider the main glass-forming components of the enamels (alkalis — Na and K, alkaline earth components – Ca and Mg, lead, and silica) as well as auxiliary materials (colorants, opacifiers, and decolorizers).

OBJECTS

The objects of this study are three Old Russian bronze items with enamel images: a pendant-icon, a temporal pendant, and a cross.

The bronze temporal pendant, decorated on both sides with multicolored enamel designs (Fig. 1), was discovered in 2004 during excavations at the site of the present-day Trading Rows in one of the historic districts of Vladimir — New Town — within the estate of a wealthy household from the mid-12th to early 13th century. It was found in an under-hearth pit of a log-frame house. The find was published by the excavation director, T.F. Mukhina [6, P. 147–149], and was later studied using a set of non-destructive methods [7].

The bronze pectoral cross, featuring multicolored enamels on both sides (Fig. 2), was discovered by T.F. Mukhina in 2008 in Vladimir during excavations at 15 Devicheskaya Street. It was found in a redeposited layer above a group of Old Russian pits (find no. 181) and is dated to the 12th–13th centuries.

The bronze pendant-icon, decorated with enamel images on both sides (Fig. 3), was discovered in 2018 during excavations by the Suzdal Expedition of the Institute of Archaeology of the Russian Academy of Sciences at the Semenovskoe-Sovetskoe 3 settlement, located 20 km from Suzdal, in the plow layer. The find is dated to the 12th–first half of the 13th century [8] and was studied using a set of non-destructive methods [9, 10].

The studied objects feature enamels of various colors. The temporal pendant has eight: deep-blue, white, turquoise, red-brown, gray, brown, green (?), and yellow. The first three colors appear on both the front and back sides, yellow only on the back, and the rest only on the front.

The pendant-icon was decorated with enamels in six colors: deep-blue, red-brown, white, gray, light gray, black, and blue-green. White and light gray are only on the front, blue-green only on the back, and the rest on both sides.

The cross features four colors: deep-blue, white, red-brown, and green. White appears on both sides, green only on the back, and the others only on the front.

Among all these colors, deep-blue, red-brown, and white are present on all three objects. Gray enamel appears on two – the temporal pendant and the pendant-icon – as does green, which is found on the temporal pendant and the cross. The remaining colors are unique to individual objects: turquoise, yellow, and brown on the temporal pendant; blue-green, light gray, and black on the pendant-icon.

METHODS AND MATERIALS

The studies of the elemental composition of enamels were carried out using scientific equipment of the Collective Use Center "Research Chemical-Analytical Center of the National Research Center "Kurchatov Institute".

The analysis of the enamels on the temporal pendant and cross was performed using inductively coupled plasma atomic emission spectroscopy with laser ablation sampling (**ICP-AES-LA**). The study was conducted on an iCAP6300 Duo atomic emission spectrometer (Thermo Fisher Scientific) with an NWR 213 laser ablation system (New Wave Research). The enamel composition was determined based on two to six measurements for each area studied. The results are presented in Tables 1–4.

Initially, the same ICP-AES-LA method was chosen for analyzing the composition of the pendant-icon. However, several challenges arose during the analysis, including significant surface leaching, high porosity of certain surfaces, and the presence of numerous pigment inclusions. As a result, the surface data showed poor reproducibility.

To assess surface homogeneity and obtain additional statistical data, a semi-quantitative electron probe microanalysis with energy-dispersive detection was performed on areas that had been pre-cleaned using laser ablation. The results from these areas demonstrated satisfactory reproducibility and revealed significant differences in surface and bulk composition. The study was conducted using a Jeol JSM-7100F scanning electron microscope (Japan) with an OXFORD INSTRUMENTS X-Max elemental analysis detector (UK). Data processing was performed using the AZtec software, version 3.1. Since applying a conductive coating to the analyzed object was not permissible, the measurements were conducted in low-vacuum mode with a residual pressure of 30 Pa. The working distance was 10 mm, and the accelerating voltage was 20 kV. The sum of the oxide forms of the elements was normalized to 100 %. The enamel composition was determined based on two to eight measurements per analyzed area. The results are presented in Tables 5 and 6.

The distribution of elements across the surface of prepared samples was studied using large-scale X-ray fluorescence mapping (XRF) at the Collective Use Center "Structural Diagnostics of Materials" of the Kurchatov Complex of Crystallography and Photonics at the National Research Center "Kurchatov Institute". The study was conducted using an ORBIS micro-XRF (EDAX) system with an X-ray tube featuring a rhodium anode. Measurements were performed in vacuum. Before mapping, an integral elemental composition analysis of the enamels was conducted using a wide beam with a 2 mm diameter. The elemental composition in the two-dimensional mapping mode was analyzed along the surface plane of the sample, with a beam diameter of 30 μm, a mapping step of 50 μm, and a spectrum accumulation time of 3000 ms per point in "live time mode". Fluorescence intensity maps for key

Fig. 1. Temporal pendant from Vladimir: a – front side, b – back side. Photo by E.S. Kovalenko, E.K. Stolyarova. Drawing by A.S. Dementyeva. The numbers indicate the analysis zones.

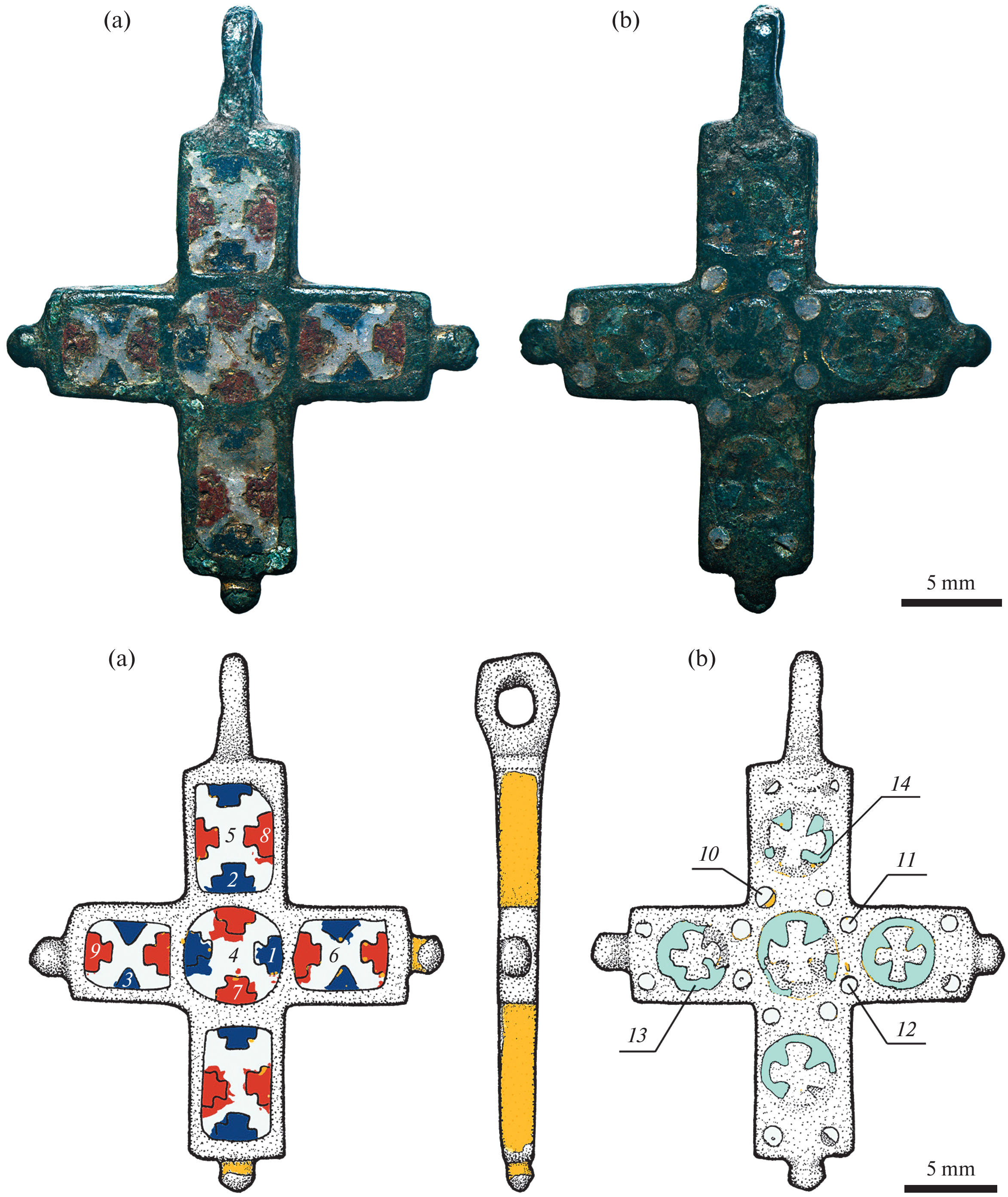

Fig. 2. The cross from Vladimir: a – front side, b – back side. Photo by E.S. Kovalenko, E.K. Stolyarova. Drawing by A.S. Dementyeva. The numbers indicate the analysis zones.

elements (Si*K*, Ca*K*, Mn*K*, Fe*K*, Co*K*, Cu*K*, Pb*L*, Sn*L*) are presented in Figures 4 and 5.

The interpretation of the results was based on the methodology of Yu.L. Shchapova [11, P. 93–108; 12, P. 87, 88, 93] and T. Stavyarskaya [13, P. 24–27], with clarifications from one of the authors of this study [14, P. 407]. This methodology determines the source of alkalis (mineral soda, plant ash, or potash) in glass and enamels by analyzing the Na_2O/K_2O ratio, as different glass compositions have distinct values. Based on calculations, Yu.L. Shchapova established that for glasses with a predominance of sodium over potassium, a Na_2O/K_2O ratio $\leqslant 13$ corresponds to glasses made from the ash of

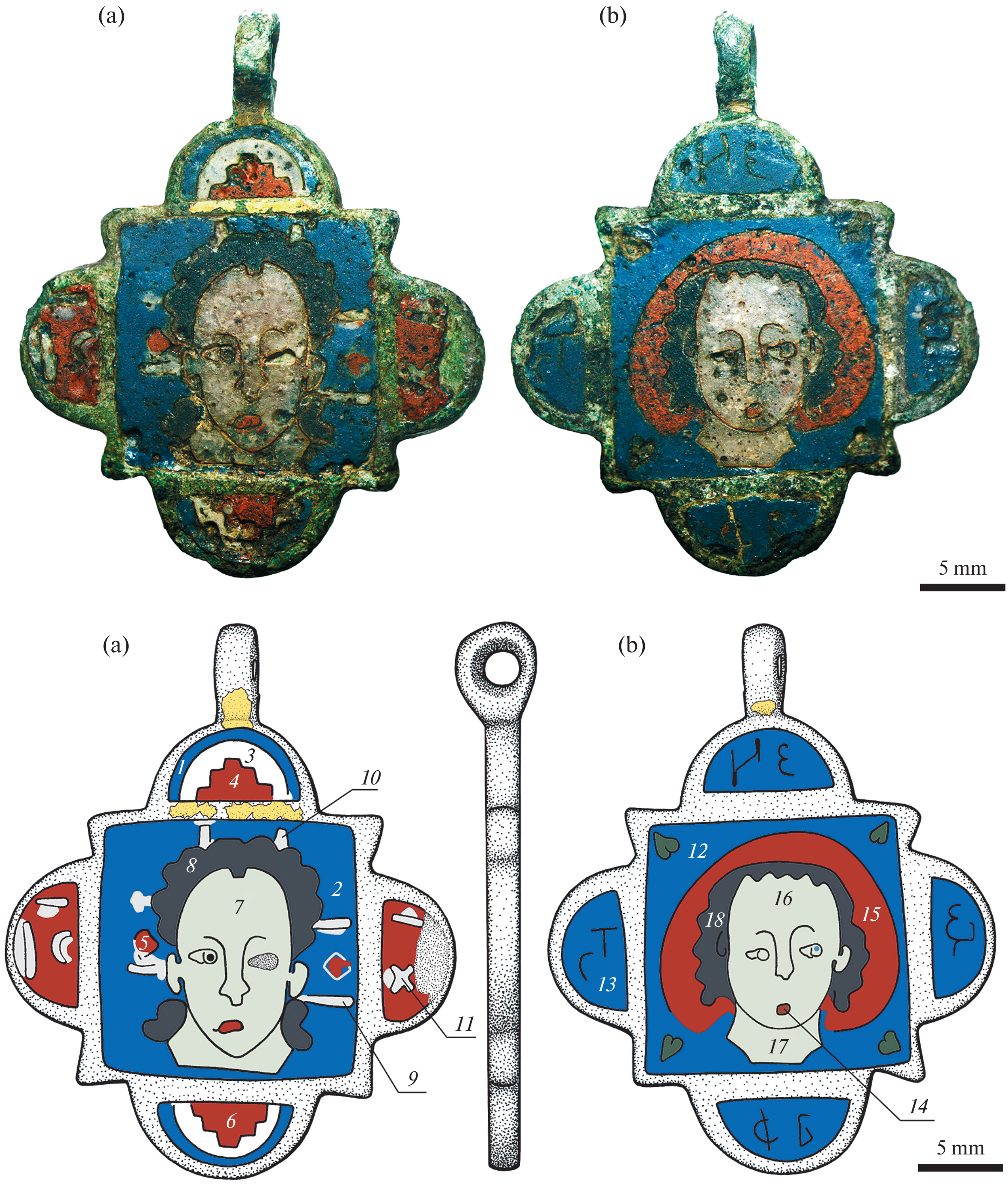

Fig. 3. Pendant-icon from the settlement of Semenovskoye-Sovetskoye 3: a – front side, b – back side. Photo by E.S. Kovalenko Drawing by A.S. Dementyeva. The numbers indicate the zones of analysis.

desert plants (halophytes). A Na_2O/K_2O ratio > 13 characterizes glasses made from mineral soda, provided that the potassium oxide content is less than 1.5 %. In cases where potassium predominates over sodium, the glass was made using the ash of temperate-zone plants or potash.

T. Stavyarskaya proposed another approach for determining the alkali source, calculating the relative potassium oxide content (C) in the total alkali content: $C = 100 \times K_2O/R_2O$. If $C < 7.1$, the alkali source was soda; if it was between 7.9 and 50, the source was desert plant ash. Furthermore, this indicator can distinguish

Table 1. Results of the study of the elemental composition of the enamels of the front side of the temporal pendant using the ICP-AES-LA method

Color	Deep-blue						White			Turquoise		Red-brown				
Analysis area*	1			2	3	4	5			6	7	8	9	10	11	12
SiO_2	*49.4*	65.4	59.7	60.0	65.0	57.9	69.6	70.3	70.0	55.1	54.0	66.1	65.3	62.4	66.3	69.9
Al_2O_3	*2.89*	1.56	1.95	1.70	1.72	2.89	2.49	2.50	2.49	2.49	1.79	2.33	2.29	2.37	2.25	2.53
B_2O_3	*0.009*	0.022	0.011	0.028	0.021	0.046	0.043	0.047	0.040	0.028	0.038	0.122	0.120	0.110	0.115	0.040
BaO	*0.069*	0.025	0.031	0.030	0.028	0.022	0.022	0.023	0.021	0.029	0.020	0.027	0.026	0.026	0.026	0.021
CaO	6.71	7.97	7.53	7.80	7.85	4.29	7.70	7.66	7.78	5.74	5.91	7.74	7.77	7.11	7.72	8.00
CoO	*0.170*	0.479	0.370	0.622	0.376	0.005	0.001	–0.001	–0.001	0.018	0.017	0.004	0.003	0.004	0.003	–0.001
Cr_2O_3	*0.003*	0.001	–0.002	0.003	–0.001	0.003	–0.001	–0.001	–0.001	0.001	0.001	0.002	0.004	0.003	0.004	0.002
CuO	*11.180*	0.021	1.152	1.705	0.067	1.532	0.582	0.128	0.425	2.766	2.209	1.865	2.998	2.377	1.499	0.118
Fe_2O_3	*6.95*	1.10	2.65	4.94	1.27	1.01	0.42	0.52	0.42	1.28	1.04	4.34	4.24	5.25	4.34	0.45
K_2O	1.68	1.99	1.99	1.87	2.02	0.96	0.95	0.62	0.51	0.17	1.93	1.60	1.53	1.51	1.53	0.50
MgO	*1.65*	2.66	2.41	2.46	2.63	0.45	0.57	0.71	0.56	2.00	1.83	2.09	2.08	1.93	2.09	0.55
MnO	*0.487*	0.623	0.582	0.584	0.612	0.139	0.077	0.080	0.078	0.253	0.265	0.687	0.691	0.650	0.690	0.077
MoO	*0.001*	–0.001	0.002	0.001	–0.001	–0.001	0.003	–0.001	–0.001	0.002	–0.001	0.001	–0.001	0.001	0.002	0.002
Na_2O	*7.5*	11.9	9.9	10.3	11.5	12.5	12.7	12.4	13.5	8.6	9.8	12.7	12.6	12.0	12.9	12.8
NiO	0.016	–0.003	0.012	–0.003	0.001	0.001	–0.006	–0.003	–0.007	0.002	0.001	–0.002	–0.001	0.003	–0.001	–0.005
PbO	*8.22*	4.78	9.38	5.83	5.08	17.20	0.47	0.25	0.03	16.90	18.43	0.29	0.25	3.88	0.24	0.04
Sb_2O_3	*0.18*	0.10	0.12	0.12	0.10	0.59	4.16	4.51	4.03	0.02	0.01	0.01	0.01	0.02	0.02	4.85
SnO	*1.80*	1.36	1.73	1.62	1.56	0.13	–0.001	0.02	–0.001	2.89	2.38	0.02	0.03	0.05	0.05	–0.001
SrO	*0.081*	0.055	0.057	0.056	0.055	0.034	0.047	0.048	0.048	0.043	0.042	0.079	0.080	0.072	0.079	0.050
TiO_2	0.078	0.068	0.074	0.079	0.074	0.104	0.057	0.059	0.057	0.106	0.078	0.122	0.118	0.122	0.118	0.056
V_2O_5	*0.012*	0.003	0.007	0.004	0.004	0.003	0.003	0.005	0.002	0.005	0.004	0.005	0.005	0.005	0.005	0.004
ZnO	*0.925*	0.011	0.259	0.254	0.017	0.044	0.007	0.016	0.006	0.097	0.106	0.032	0.033	0.101	0.026	0.009

End of Table 1

Color	Grey				Green (?)		Brown		
Analysis area*	13				14		15		
SiO_2	74.1	*61.7*	*59.6*	*63.8*	*47.3*	*38.7*	*62.3*	*61.6*	*63.4*
Al_2O_3	2.14	*0.99*	*0.87*	*1.13*	*7.08*	*8.19*	*0.85*	*0.79*	*0.77*
B_2O_3	0.066	*0.035*	*0.030*	*0.038*	*0.007*	0.065	0.025	0.021	0.024
BaO	0.017	*0.014*	*0.014*	*0.015*	*0.042*	*0.066*	*0.015*	*0.016*	*0.015*
CaO	6.01	*1.70*	*1.23*	*2.04*	*2.51*	*4.22*	*0.37*	*0.45*	*0.36*
CoO	–0.001	*0.001*	*–0.001*	*0.001*	*–0.005*	–0.010	–0.001	0.001	–0.001
Cr_2O_3	0.001	*–0.001*	*0.001*	*–0.001*	*0.006*	*0.026*	*0.001*	*0.002*	*0.002*
CuO	0.052	*–0.096*	*0.015*	*0.313*	*3.295*	*5.496*	*0.817*	*3.539*	*0.382*
Fe_2O_3	0.67	*0.42*	*0.42*	*0.49*	*6.70*	*17.13*	2.02	1.16	0.85
K_2O	0.55	*4.21*	*6.07*	*1.77*	*1.74*	*3.34*	*0.67*	*0.23*	*0.32*
MgO	0.68	0.18	0.16	0.40	0.64	1.47	0.09	0.30	0.13
MnO	0.084	*0.688*	*0.874*	*0.720*	*0.222*	*0.386*	*0.998*	1.020	1.032
MoO	–0.001	*0.002*	*0.003*	*0.004*	*0.001*	*–0.001*	*0.003*	*0.003*	*0.004*
Na_2O	14.4	*9.5*	8.0	9.7	0.3	–0.1	0.1	–0.1	–0.2
NiO	–0.001	*–0.002*	*0.003*	*0.001*	*0.001*	*0.005*	*–0.001*	0.002	–0.003
PbO	0.31	*21.04*	*22.95*	*18.98*	*29.34*	*20.67*	*31.48*	*30.67*	*32.41*
Sb_2O_3	0.78	*0.14*	*0.08*	0.36	0.01	0.03	0.01	–0.001	–0.001
SnO	0.02	*–0.001*	*0.01*	*0.03*	*–0.001*	*–0.01*	*0.01*	*0.03*	0.03
SrO	0.052	*0.021*	*0.018*	*0.024*	*0.026*	*0.041*	*0.012*	*0.012*	*0.012*
TiO_2	0.070	*0.097*	*0.104*	*0.108*	0.241	0.203	0.120	0.125	0.125
V_2O_5	0.003	*0.004*	*0.004*	*0.005*	*0.019*	*0.034*	*0.007*	*0.009*	*0.006*
ZnO	0.009	*0.005*	0.011	0.032	0.314	0.467	0.047	0.062	0.037

Note: Italics denote results excluded from interpretation.
*The numbers of the analysis zones correspond to the numbers in Fig. 1.

Table 2. Results of the study of the elemental composition of the enamels on the reverse side of the temporal pendant using the ICP- AES-LA method

Color	Deep-blue			White			Turquoise			Yellow	
Analysis area*	16			17			18			19	20
SiO_2	64.9	67.9	67.9	68.5	71.1	68.7	*72.0*	64.7	65.6	65.8	65.5
Al_2O_3	2.50	2.31	2.37	2.03	2.26	2.19	*2.63*	2.55	2.27	2.05	2.21
B_2O_3	0.053	0.027	0.037	0.056	0.074	0.044	*0.054*	0.073	0.052	0.058	0.049
BaO	0.027	0.027	0.028	0.022	0.022	0.021	*0.017*	0.031	0.016	0.020	0.021
CaO	7.90	6.67	6.65	6.15	6.04	6.47	*6.16*	6.72	6.69	5.30	5.06
CoO	0.248	0.245	0.195	0.001	–0.001	–0.001	*–0.001*	0.001	0.002	0.001	–0.001
Cr_2O_3	–0.001	–0.001	0.003	0.002	0.002	0.001	*0.003*	–0.001	0.001	–0.001	0.006
CuO	0.290	0.402	0.398	0.579	0.211	0.127	*2.504*	2.261	2.315	1.062	0.133
Fe_2O_3	1.56	1.47	1.24	0.57	0.69	0.51	*0.91*	0.76	0.67	0.45	1.13
K_2O	0.71	0.80	0.68	0.64	0.77	0.77	*1.11*	1.46	1.17	0.86	0.67
MgO	0.60	0.52	0.54	1.23	0.60	1.06	*0.66*	0.73	0.65	0.41	0.47
MnO	0.514	0.782	0.837	0.357	0.199	0.245	*0.044*	0.039	0.049	0.158	0.356
MoO	0.004	0.002	–0.001	0.002	–0.002	0.001	*0.001*	0.001	0.002	0.001	–0.001
Na_2O	15.3	14.5	15.2	16.4	16.0	16.6	*11.7*	17.6	17.4	16.3	15.6
NiO	0.002	0.006	0.005	–0.003	0.002	–0.003	*0.001*	0.001	–0.002	0.001	0.001
PbO	0.34	1.17	1.26	1.94	0.09	0.20	*0.25*	0.55	0.18	6.81	7.72
Sb_2O_3	4.95	2.99	2.56	1.36	1.78	2.90	*1.57*	2.17	2.06	0.53	0.81
SnO	0.01	0.02	0.01	0.01	0.02	0.01	*0.07*	0.09	0.58	0.03	0.05
SrO	0.052	0.052	0.051	0.048	0.050	0.049	*0.070*	0.058	0.080	0.043	0.039
TiO_2	0.058	0.059	0.061	0.079	0.084	0.072	*0.151*	0.141	0.121	0.066	0.109
V_2O_5	0.002	0.003	0.002	0.001	0.001	0.002	*0.001*	0.001	0.001	0.003	0.002
ZnO	0.016	0.018	0.008	0.010	0.011	0.008	*0.114*	0.101	0.131	0.006	0.005

Note: Italics denote results excluded from interpretation.
*The numbers of the analysis zones correspond to the numbers in Fig. 1.

Table 3. Results of the study of the elemental composition of the enamels of the front side of the cross using the ICP-AES-LA method

Color	Deep-blue			White			Red-brown		
Analysis area*	1	2	3	4	5	6	7	8	9
SiO_2	63.3	64.4	61.6	66.8	67.0	67.9	64.7	64.9	64.2
Al_2O_3	1.63	1.70	1.74	2.43	2.24	2.29	2.54	1.87	2.61
B_2O_3	0.042	0.041	0.037	0.051	0.054	0.057	0.178	0.272	0.171
BaO	0.028	0.027	0.030	0.023	0.028	0.024	0.050	0.169	0.060
CaO	7.73	7.47	7.40	6.93	6.71	6.57	7.70	8.90	7.74
CoO	0.282	0.227	0.258	0.003	0.006	0.002	0.004	–0.001	0.002
Cr_2O_3	0.004	0.002	0.005	0.001	-0.001	0.001	0.003	0.003	0.003
CuO	0.159	0.151	0.742	0.121	0.404	0.178	1.320	1.550	1.849
Fe_2O_3	1.44	1.24	2.98	0.64	0.58	0.49	4.04	3.23	4.14
K_2O	1.85	2.09	2.03	0.89	0.89	0.90	2.14	1.90	2.03
MgO	2.38	2.26	2.42	1.43	1.79	1.05	2.07	2.51	2.05
MnO	0.601	0.566	0.585	0.231	0.133	0.201	0.793	1.214	0.829
MoO	–0.001	–0.002	0.003	–0.001	–0.003	–0.001	0.001	–0.002	–0.001
Na_2O	13.4	13.8	12.9	15.5	15.5	16.1	13.3	12.8	12.6
NiO	–0.002	0.002	0.005	–0.002	0.001	-0.003	0.006	0.004	0.008
PbO	5.62	4.17	5.21	0.60	0.42	0.29	0.80	0.53	1.07
Sb_2O_3	0.58	0.74	0.55	4.09	4.19	3.72	0.26	0.20	0.10
SnO	1.18	0.90	1.17	0.11	0.07	0.04	0.05	0.08	0.16
SrO	0.056	0.056	0.055	0.052	0.052	0.050	0.115	0.150	0.115
TiO_2	0.075	0.075	0.082	0.072	0.079	0.068	0.141	0.100	0.154
V_2O_5	0.003	0.001	0.001	0.002	0.001	0.001	0.004	0.002	0.004
ZnO	0.017	0.017	0.032	0.016	0.033	0.014	0.024	0.024	0.047

Note:*The numbers of the analysis zones correspond to the numbers in Fig. 2.

Table 4. Results of the study of the elemental composition of the enamels on the reverse side of the cross using the ICP-AES-LA method

Color	White			Green	
Analysis area*	10	11	12	13	14
SiO_2	66.9	68.2	*45.5*	54.7	62.8
Al_2O_3	2.32	2.33	*1.74*	2.77	2.67
B_2O_3	0.051	0.050	*0.030*	0.029	0.034
BaO	0.024	0.022	*0.099*	0.060	0.025
CaO	6.85	6.06	*7.39*	6.87	6.91
CoO	–0.001	0.002	*0.001*	–0.001	0.002
Cr_2O_3	0.001	–0.001	*0.001*	0.001	0.001
CuO	0.165	0.152	*18.540*	6.162	0.984
Fe_2O_3	0.56	0.51	*0.49*	0.84	0.48
K_2O	0.80	0.70	*0.89*	0.81	0.65
MgO	1.46	1.33	*1.04*	0.51	0.57
MnO	0.259	0.142	*0.128*	0.086	0.122
MoO	0.002	0.001	*0.004*	0.001	0.002
Na2O	14.8	16.5	*10.6*	11.9	14.2
NiO	–0.008	–0.001	*0.003*	0.009	0.001
PbO	1.06	0.23	*4.82*	13.49	9.88
Sb_2O_3	4.47	3.60	*3.15*	0.07	0.02
SnO	0.10	0.03	*5.05*	1.26	0.51
SrO	0.052	0.052	*0.072*	0.056	0.050
TiO_2	0.074	0.079	*0.053*	0.074	0.071
V_2O_5	0.003	0.002	*0.007*	0.002	0.002
ZnO	0.016	0.021	*0.268*	0.133	0.012

Note: Italics denote results excluded from interpretation.
*The numbers of the analysis zones correspond to the numbers in Fig. 2.

different plant species (e.g., *Kalidium caspicum* or *Salicornia herbacea*) and their parts (aerial parts or roots).

According to her, when the relative potassium oxide content falls between 7.1 and 7.9, it is impossible to determine whether soda or ash was used, placing such glasses in an "uncertain zone". By applying both methodologies (Yu.L. Shchapova and T. Stavyarskaya), one of the authors of this study processed a dataset of over 300 chemical analyses of ancient and medieval glasses. The results showed that for glasses with $Na_2O/K_2O \leqslant 13$, the relative potassium oxide content ranged from 7.3 to 7.9 ($7.3 \leqslant C < 7.9$), indicating the use of plant ash. This finding reduces the uncertainty in identifying the alkali source [14, P. 407].

T. Stavyarskaya also developed guidelines for determining the source of alkaline-earth raw materials. This involves calculating the relative magnesium oxide content (a) in the total alkaline-earth content: $a = 100 \times MgO/RO$. If $a \leqslant 7.5$, the calcium-magnesium raw material source was limestone; if $7.5 < a \leqslant 22$, the source was dolomitic limestone; if $a > 22$, it was dolomite.

The understanding of glassmaking as an organized and regulated production process, which followed strict rules for combining components and had limited raw material choices, led Yu.L. Shchapova to introduce the concept of a "recipe norm" ($N = Na_2O + K_2O/CaO + MgO$). This represents a quantitative characteristic of ancient glasses related to the combination rules for alkali and alkaline-earth raw materials. In cases of low alkaline-earth content and high lead content, the recipe norm is calculated using the formula: $1.6 \times (Na_2O + K_2O)/PbO$. Through calculations, these norms were identified, grouping around values between 0.3 and 5, with deviations never exceeding 10 %.

A set of recipe norms, corresponding to different types of alkali sources, was established for each glassmaking tradition. For example, the Roman tradition generally used soda, with metropolitan glassmakers favoring a norm of 3, while provincial Roman glassmakers used norms of 2 and 2.5. Plant ash was used in the inland regions of the Near East, particularly in Mesopotamia, where norms of 1.25 and 1.5 were applied, while the Syrian tradition adhered to norms of 1.5, 2, and 2.5 [15, P. 87, 106, 122, 127, 128]. The Byzantine tradition used both soda and plant ash, primarily following norms of 1, 1.25, 1.5, and 2 [16, P. 94, 95].

RESULTS

Let us examine the results of the study on the chemical composition of the enamels (Tables 7–12). We assume that the enamel in a given area should have had a uniform composition. Therefore, results indicating significant heterogeneity were excluded from

Table 5. Results of the study of the elemental composition of the enamels of the front side of the pendant-icon using the SEM/ESM method (oxides, wt.%)

Color	Analysis area*		Na	Mg	Al	Si	P	S	Cl	K	Ca	Ti	Cr	Mn	Fe	Co	Ni	Cu	Zn	Sn	Sb	Pb
Deep-blue	1	Spectrum 253	10.39	2.74	1.74	57.40	0.29	0.00	0.75	1.94	6.73	0.18	0.07	0.59	1.65	0.28	0.08	0.40	0.15	5.17	0.00	9.45
		Spectrum 254	10.38	2.76	1.62	57.31	0.30	0.02	0.89	1.96	7.07	0.27	0.09	0.61	1.76	0.38	0.00	0.54	0.07	4.70	0.00	9.26
		Spectrum 255	10.13	2.75	1.87	57.15	0.32	0.12	0.83	2.23	7.09	0.22	0.00	0.52	1.81	0.41	0.06	0.33	0.05	4.91	0.00	9.21
	2	Spectrum 256	10.43	2.77	1.19	57.76	0.29	0.00	0.68	1.87	7.57	0.11	0.03	0.59	2.19	0.52	0.11	0.17	0.00	4.90	0.00	8.81
		Spectrum 257	10.32	2.73	1.17	58.19	0.24	0.00	0.68	1.90	7.29	0.01	0.06	0.67	2.14	0.35	0.00	0.07	0.06	5.03	0.00	9.08
		Spectrum 258	*9.26*	*2.7*	*2.11*	*56.12*	*0.49*	*0.17*	*1.16*	*2.53*	*7.03*	*0.49*	*0.05*	*0.56*	*2.55*	*0.39*	*0.03*	*0.49*	*0*	*5.15*	*0*	*8.73*
		Spectrum 259	10.57	2.92	1.14	57.94	0.12	0.00	0.70	1.97	7.26	0.02	0.00	0.63	2.00	0.45	0.03	0.12	0.09	4.98	0.00	9.07
		Spectrum 260	10.57	2.67	1.20	57.52	0.37	0.00	0.65	2.06	7.32	0.07	0.00	0.65	2.00	0.39	0.00	0.16	0.15	5.14	0.00	9.08
		Spectrum 261	10.06	2.71	1.71	57.42	0.28	0.02	0.80	1.99	7.12	0.23	0.00	0.73	2.03	0.37	0.00	0.13	0.08	5.37	0.00	8.96
White	3	Spectrum 245	13.87	1.73	1.68	60.11	0.23	0.09	0.82	1.51	6.36	0.06	0.02	0.51	0.48	0.00	0.00	0.64	0.14	5.97	0.48	5.31
		Spectrum 246	14.22	1.39	1.90	63.03	0.19	0.10	0.82	1.67	6.50	0.13	0.05	0.47	0.48	0.00	0.05	1.45	0.00	1.93	0.85	4.78
		Spectrum 248	11.15	2.06	3.07	59.62	0.45	0.10	1.24	2.04	6.69	0.38	0.00	0.54	1.21	0.10	0.11	0.46	0.00	3.40	0.48	6.90
		Spectrum 250	13.49	0.63	2.07	66.98	0.15	0.47	0.98	2.02	7.27	0.09	0.00	0.33	0.72	0.03	0.08	0.68	0.05	0.39	1.61	1.97
		Spectrum 251	12.66	1.01	2.56	64.60	0.14	0.35	0.89	2.04	7.09	0.16	0.03	0.38	0.95	0.01	0.06	0.26	0.00	0.78	1.53	4.49
		Spectrum 252	*6.68*	*0.89*	*2.97*	*70.37*	*0.35*	*0.47*	*1.14*	*2.4*	*7.09*	*0.35*	*0*	*0.41*	*1.11*	*0*	*0.03*	*0.54*	*0.07*	*0.73*	*1.64*	*2.74*
Red-brown	4	Spectrum 237	12.29	2.26	3.23	63.86	0.36	0.33	0.93	2.29	8.03	0.46	0.02	0.94	3.16	0.00	0.05	1.13	0.06	0.18	0.00	0.42
		Spectrum 238	12.27	2.26	3.47	63.38	0.44	0.23	0.90	2.28	7.90	0.45	0.00	0.90	3.46	0.05	0.00	1.34	0.07	0.17	0.00	0.42
		Spectrum 239	11.77	2.23	3.35	62.29	0.45	0.40	0.93	2.46	7.98	0.66	0.08	0.89	3.73	0.00	0.07	1.41	0.06	0.30	0.00	0.93
	5	Spectrum 281	13.76	2.15	2.62	64.06	0.33	0.05	0.83	2.00	7.74	0.23	0.08	1.22	3.32	0.02	0.00	1.07	0.01	0.00	0.00	0.51
		Spectrum 282	13.63	2.20	2.39	63.72	0.29	0.20	0.72	1.96	8.24	0.22	0.07	1.08	3.24	0.06	0.00	1.26	0.00	0.00	0.00	0.73
		Spectrum 283	12.09	1.90	3.29	63.71	0.55	0.28	0.95	2.39	7.44	0.49	0.00	1.15	3.65	0.01	0.00	1.18	0.13	0.18	0.00	0.63
		Spectrum 284	11.90	2.12	3.26	63.46	0.55	0.42	0.91	2.35	8.10	0.48	0.01	1.00	3.11	0.10	0.00	1.44	0.12	0.26	0.00	0.40
	6	Spectrum 286	14.22	2.22	2.72	63.82	0.39	0.11	0.74	1.85	7.74	0.18	0.00	1.10	3.19	0.00	0.00	1.28	0.08	0.00	0.00	0.37
		Spectrum 287	*14.59*	*1.85*	*3.39*	*61.9*	*0.42*	*0.16*	*0.89*	*1.92*	*5.85*	*0.32*	*0.02*	*2.15*	*4.65*	*0.06*	*0.08*	*1.33*	*0*	*0*	*0*	*0.43*
		Spectrum 288	10.76	1.50	4.74	62.38	0.60	0.12	0.85	2.68	6.43	0.47	0.09	2.01	4.93	0.01	0.09	1.54	0.08	0.00	0.14	0.57
		Spectrum 289	11.88	1.98	4.25	61.93	0.56	0.39	1.09	2.42	7.06	0.96	0.03	1.37	3.99	0.00	0.00	1.14	0.20	0.25	0.04	0.47

End of Table 5

Color	Analysis area*		Na	Mg	Al	Si	P	S	Cl	K	Ca	Ti	Cr	Mn	Fe	Co	Ni	Cu	Zn	Sn	Sb	Pb
Grey	7	Spectrum 262	17.00	0.79	2.09	69.11	0.08	0.33	0.98	0.77	6.51	0.19	0.00	0.60	0.87	0.00	0.02	0.02	0.00	0.06	0.56	0.02
		Spectrum 263	16.18	0.70	2.09	69.59	0.14	0.32	1.11	0.84	6.29	0.15	0.02	1.02	0.67	0.01	0.04	0.15	0.02	0.00	0.29	0.35
		Spectrum 264	*1.48*	*0.81*	2.73	82.98	0.13	0.57	1.10	1.55	5.71	0.29	0	0.1	1.02	0	0.06	0.16	0.03	0.02	0.99	0.27
		Spectrum 265	1.94	0.9	2.73	81.16	0.15	0.46	1.20	1.38	6.71	0.33	0	0.5	1.25	0	0	0.16	0	0.09	0.54	0.48
		Spectrum 266	15.83	0.63	2.14	70.94	0.01	0.31	1.14	0.73	6.72	0.14	0.00	0.11	0.89	0.00	0.00	0.00	0.07	0.00	0.18	0.16
		Spectrum 267	16.38	0.60	2.04	69.77	0.08	0.40	1.12	0.84	6.79	0.07	0.00	0.15	0.71	0.00	0.00	0.01	0.00	0.04	0.91	0.09
		Spectrum 268	*3.17*	*0.77*	*2.58*	*80.02*	*0.34*	*0.59*	*1.25*	*1.47*	*6.73*	*0.36*	*0.07*	*0.28*	*1.15*	*0*	0	0.21	0.08	0.11	0.65	0.19
		Spectrum 269	3.16	1.16	2.79	79.53	0.21	0.54	1.23	1.48	6.33	0.38	0.13	0.06	*1.26*	*0.14*	*0*	*0.22*	*0.02*	*0.08*	*0.97*	*0.31*
Black	8	Spectrum 274	10.94	2.57	1.92	64.52	0.19	0.24	0.89	6.28	8.50	0.15	0.09	2.26	0.66	0.05	0.01	0.26	0.01	0.00	0.00	0.47
		Spectrum 275	11.24	2.48	2.16	64.11	0.32	0.10	0.81	4.96	8.07	0.23	0.00	2.85	1.06	0.00	0.00	0.90	0.03	0.00	0.03	0.62
		Spectrum 276	*10.72*	*1.64*	*3.4*	*63.73*	*0.45*	*0.29*	*0.95*	*4.42*	*7.21*	*0.46*	*0.03*	*4.11*	*1.43*	*0*	*0*	*0.34*	*0.17*	*0.05*	*0*	*0.62*
		Spectrum 277	12.00	1.18	3.76	65.67	0.40	0.11	0.90	3.77	6.01	0.31	0.04	3.83	1.27	0.00	0.09	0.19	0.11	0.00	0.00	0.37
		Spectrum 278	12.46	1.53	3.93	63.63	0.37	0.18	0.59	3.73	5.94	0.26	0.01	5.04	1.48	0.00	0.07	0.17	0.00	0.00	0.02	0.58
		Spectrum 279	10.78	1.62	4.01	63.75	0.33	0.29	0.90	4.7	6.51	0.51	0.06	4.13	1.51	0.02	0	0.19	0	0	0	0.67
		Spectrum 280	11.05	1.34	4.14	65.8	0.42	0.22	0.74	4.22	6.23	0.41	0.01	3.31	1.42	0.01	0	0.23	0	0	0	0.47
Light grey	9	*Spectrum 270*	*9.79*	*2.34*	*1.94*	*56.35*	*0.52*	*0.2*	*0.95*	*1.99*	*7.02*	*0.64*	*0.04*	*0.51*	*1.01*	*0.01*	*0.02*	*1.85*	*0.18*	*5.56*	*0.13*	*8.98*
		Spectrum 271	*9.9*	*2.19*	*2.12*	*61.31*	*0.49*	*0.37*	*1.15*	*2.06*	*6.97*	*0.66*	*0.03*	*0.46*	*0.9*	*0.1*	*0*	*0.69*	*0.1*	*3.58*	*0.69*	*6.24*
	10	Spectrum 272	11.04	2.26	1.72	57.67	0.47	0.19	1.03	1.99	6.84	0.53	0.04	0.59	4.77	0.16	0.02	0.96	0.06	3.39	0.02	6.25
		Spectrum 273	*10.58*	*1.97*	*2*	*59.92*	*0.36*	*0.39*	*1.15*	*2.7*	*6.99*	*0.45*	*0.09*	*0.81*	*0.81*	*0*	*0*	*2.07*	*0.01*	*3.35*	*0.36*	*5.99*
	11	*Spectrum 290*	*5.28*	*0.89*	*0.86*	*20.4*	*0.37*	*0*	*0.28*	*0.77*	*2.23*	*0.23*	*0.41*	*0.15*	*0*	*0.18*	*0*	*1.08*	*0.43*	*62.46*	*0*	*4*
		Spectrum 291	11.96	2.45	1.55	58.10	0.43	0.00	0.79	1.33	6.90	0.15	0.05	0.60	0.57	0.09	0.02	1.33	0.22	3.99	0.00	9.48
		Spectrum 292	12.30	2.40	1.69	59.09	0.39	0.00	0.80	1.31	6.98	0.08	0.00	0.58	0.60	0.00	0.07	1.39	0.01	4.03	0.04	8.23
		Spectrum 293	11.56	2.02	2.36	60.58	0.43	0.16	1.01	1.71	6.78	0.38	0.07	0.39	0.98	0.13	0.12	1.06	0.06	3.18	0.14	6.87

Note: Italics denote results excluded from interpretation.
*The numbers of the analysis zones correspond to the numbers in Fig. 3.

Table 6. Results of the study of the elemental composition of the enamels on the reverse side of the pendant-icon using the SEM/ESM method (oxides, wt.%)

Color	Analysis area*		Na	Mg	Al	Si	P	S	Cl	K	Ca	Ti	Cr	Mn	Fe	Co	Ni	Cu	Zn	Sn	Sb	Pb
Deep-blue	12	Spectrum 319	11.00	2.77	1.34	58.16	0.32	0.00	0.73	1.89	6.79	0.11	0.00	0.60	1.81	0.51	0.02	0.00	0.00	4.61	0.00	9.34
		Spectrum 320	10.45	2.69	1.34	57.77	0.18	0.00	0.77	2.02	7.22	0.10	0.00	0.61	2.13	0.29	0.10	0.18	0.00	4.51	0.00	9.65
		Spectrum 321	*8.98*	*2.68*	*2.81*	*55.17*	*0.48*	*0.06*	*0.88*	*2.2*	*6.97*	0.38	0	0.65	5.04	0.3	0	0.34	0.26	4.61	0	8.19
		Spectrum 322	9.13	2.61	2.47	56.55	0.29	0.15	0.87	*2.23*	*6.96*	*0.21*	*0.03*	*0.64*	*2.9*	*0.49*	*0*	*0.27*	*0*	*5.47*	*0*	*8.74*
	13	Spectrum 327	11.08	2.91	1.28	57.46	0.26	0.00	0.63	1.78	7.08	0.11	0.09	0.66	1.82	0.39	0.10	0.13	0.00	4.87	0.00	9.35
		Spectrum 328	10.41	2.69	1.37	57.06	0.24	0.00	0.68	1.95	7.16	0.13	0.00	0.71	2.13	0.40	0.11	0.18	0.00	5.28	0.00	9.51
		Spectrum 329	8.9	2.51	2.45	56.56	0.5	0.01	0.89	2.35	7.05	0.56	0	0.7	2.51	0.4	0.14	0.33	0	5.08	0	9.04
		Spectrum 330	8.7	2.67	2.55	56.25	0.35	0	0.84	2.35	7	0.48	0.11	0.65	2.66	0.32	0.01	0.32	0.09	5.69	*0*	*8.99*
Red-brown	14	*Spectrum 298*	*13.71*	*1.92*	*3.25*	*63.21*	*0.37*	*0.16*	*0.90*	*2.03*	*6.29*	*0.25*	*0.07*	*1.4*	*3.45*	*0.07*	*0.01*	2.44	0.02	0.05	0	0.42
		Spectrum 299	12.48	1.51	3.34	62.45	0.47	0.17	1.01	2.34	5.89	0.22	0	2.18	4.25	0	0	3.36	0.02	0.1	0	0.22
		Spectrum 300	11.71	1.87	3.74	60.08	0.72	0.39	1.13	2.58	5.81	0.51	0.08	*1.29*	*4.64*	*0*	*0.04*	*4.44*	*0.17*	*0.31*	*0*	*0.5*
		Spectrum 301	11.31	2.05	3.20	62.51	0.43	0.42	0.89	2.27	7.59	0.39	0.04	1.01	3.51	0.01	0.04	3.93	0.15	0.00	0.00	0.25
	15	Spectrum 311	13.74	2.22	2.66	63.37	0.45	0.05	0.74	2.03	8.05	0.25	0.04	0.99	3.38	0.00	0.00	1.44	0.10	0.00	0.00	0.49
		Spectrum 312	13.76	2.13	2.81	63.41	0.34	0.23	0.75	2.12	7.98	0.22	0.00	0.96	3.27	0.00	0.00	1.36	0.06	0.19	0.00	0.43
		Spectrum 313	11.39	2.09	3.99	62.92	0.54	0.37	0.86	2.31	7.77	0.40	0.03	0.91	3.81	0.06	0.02	1.50	0.22	0.21	0.00	0.61
		Spectrum 314	11.69	2.06	4.18	62.77	0.51	0.33	0.90	2.41	7.41	0.29	0.00	0.79	3.63	0.00	0.05	1.54	0.09	0.00	0.00	1.36
Grey	16	Spectrum 294	12.80	0.61	2.23	73.12	0.02	0.39	1.14	0.80	6.77	0.10	0.02	0.46	0.72	0.05	0.08	0.06	0.00	0.00	0.50	0.14
		Spectrum 295	15.27	0.75	2.14	70.30	0.18	0.31	1.12	0.90	6.94	0.15	0.09	0.43	0.79	0.00	0.00	0.11	0.00	0.02	0.29	0.19
		Spectrum 296	*2.16*	*1.08*	*3.71*	*79.69*	*0.26*	*0.73*	*1.16*	*1.65*	*6.05*	*0.23*	*0*	*0.1*	*1.41*	0.04	0	0.12	0.03	0.12	1.45	0.02
		Spectrum 297	1.81	1.11	3.24	79.77	0.38	0.61	1.25	2	6.16	0.38	0.02	*0.15*	*1.26*	*0*	*0*	*0.2*	*0.08*	*0.12*	*1.18*	*0.27*
	17	Spectrum 302	16.62	2.17	2.20	62.48	0.70	0.16	0.99	0.81	7.55	0.12	0.02	0.51	2.42	0.01	0.00	0.37	0.00	0.05	0.00	2.82
		Spectrum 303	*8.53*	*0.88*	*2.52*	*75.38*	*0.13*	*0.35*	1.21	1.02	7.45	0.15	0	0.11	1.03	0	0.05	0.19	0.1	0	0.7	0.21
		Spectrum 304	1.37	0.84	3.33	81.45	0.36	0.57	1.14	1.85	5.07	0.29	0.01	0.18	1.17	0.08	0.06	0.35	0.08	0.11	1.07	0.61
		Spectrum 305	1.52	0.96	*3.57*	*80.07*	*0.52*	*0.72*	*1.34*	*2.38*	*4.98*	*0.31*	*0.05*	*0.37*	*1.62*	*0.02*	*0*	*0.26*	*0.03*	*0.09*	*0.86*	*0.34*
Black	18	Spectrum 307	2.16	0.21	1.09	68.23	0.23	0	0.10	3.71	0.96	0.17	0	0.3	0.37	0	0.06	0.22	0	0.08	0	22.12
		Spectrum 308	8.18	1.49	3.79	62.56	0.38	0	0.64	8.93	5.51	0.23	0	3.92	1.32	0	0	0.94	0	0.13	0.1	1.88
		Spectrum 309	2.22	0.27	1.57	68.41	0.34	0	0.27	2.34	1.23	0.24	0	0.37	0.65	0	0.08	0.23	0	0.29	0.17	21.31
		Spectrum 310	7.65	1.12	4.16	63.97	0.54	0.12	0.83	8.51	5.08	0.45	0	3.06	1.46	*0*	*0*	*0.37*	*0*	*0*	*0.08*	*2.61*
		Spectrum 315	11.27	1.71	3.62	63.88	0.38	0.15	0.71	3.95	6.96	0.28	0.02	4.17	1.31	0.00	0.05	0.21	0.19	0.00	0.00	1.14
		Spectrum 316	*11.86*	*2.41*	*2.35*	*65.23*	*0.24*	*0.19*	*0.86*	*4.06*	*8.11*	0.19	0.07	2.53	0.9	0	0	0.13	0.06	0	0	0.79
		Spectrum 317	9.46	2.2	4.11	64.36	0.61	0.26	1.06	*5.03*	*7.45*	*0.44*	*0*	*2.37*	*1.69*	*0*	*0.06*	*0.12*	*0*	*0*	*0.03*	*0.73*
		Spectrum 318	10.02	1.47	4.03	62.42	0.48	0.24	0.95	4.82	6.31	0.35	0.00	4.60	1.44	0.05	0.00	0.30	0.10	0.00	0.00	2.42

Note: Italics denote results excluded from interpretation.
*The numbers of the analysis zones correspond to the numbers in Fig. 3.

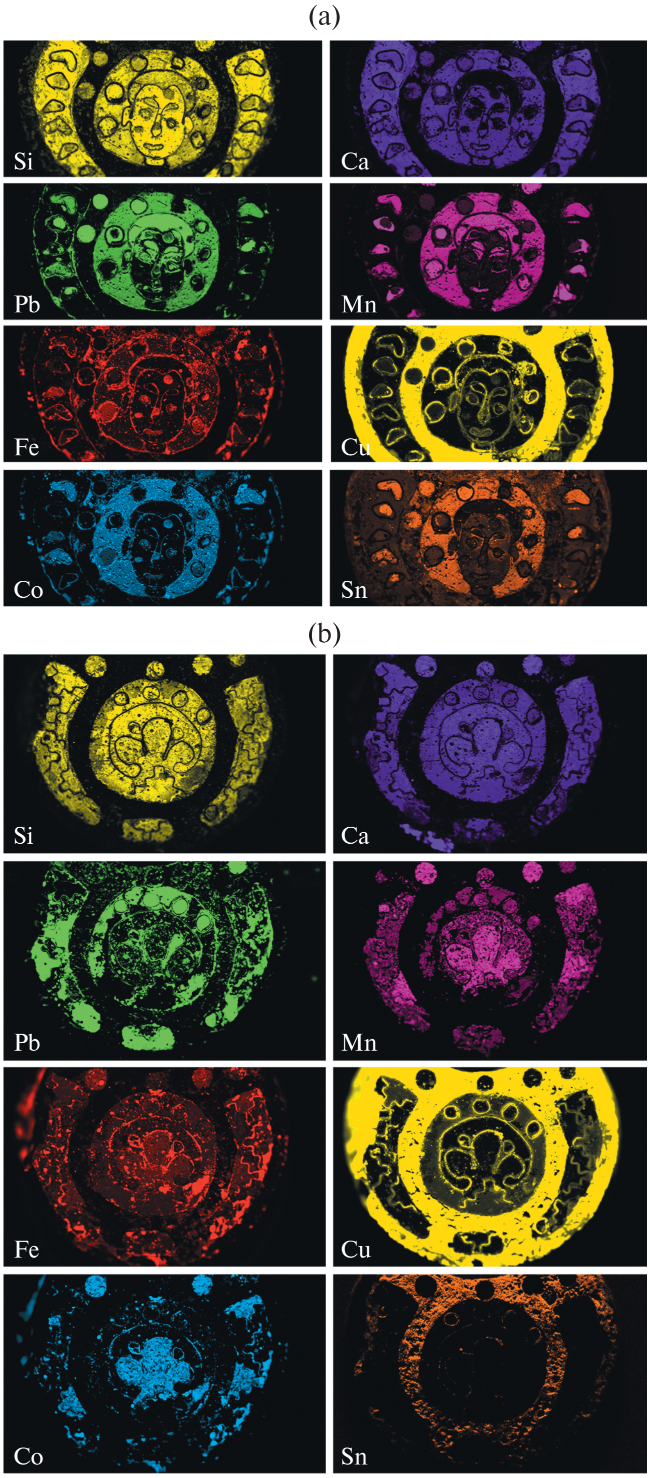

Fig. 4. Maps of the distribution of elements obtained by X-ray fluorescence mapping on the surface of the temporal pendant: a — front side, b — back side.

interpretation (they are italicized in Tables 1–6). In some cases, interpretation was based on the average values of the main glass-forming and auxiliary materials, which are italicized in Tables 7–12.

The deep-blue enamel was used on both sides of the temporal pendant, on the pendant icon, and on the front side of the cross.

The enamels on both sides of the pendant-icon (Table 7: *1*, *2*; Table 8: *12*, *13*; Fig. 3: *1*, *2*, *12*, *13*) and in certain areas of the front side of the temporal pendant (Table 9: *1–3*; Fig. 1: *1–3*; 4a) were found to be identical. A Na–Ca–Si class glass with an elevated lead oxide content (5.08–9.5 %) was used. Plant ash from arid-zone halophytes (above-ground parts of the annual plant *Kalidium caspicum*) served as the alkali source, while dolomites were used as the alkaline earth source. The components were combined at a ratio (recipe norm) of 1.25. Cobalt oxide was used as a colorant, tin oxide as an opacifier, and manganese oxide as a decolorizer. According to A.N. Galibin, cobalt-colored glass, like other colored glasses, did not require a decolorizer, as this would be unnecessary given that cobalt's coloring effect is stronger than that of iron [5, P. 30]. However, in this case, the iron content is quite high (1.7–2.7 %), which could have interfered with achieving the desired hue, necessitating the use of a decolorizer. Notably, the cobalt concentration in the enamels on both sides of the pendant-icon is high (0.36–0.44 %), as well as in the enamel on the front side of the temporal pendant (0.38–0.62 %), which likely explains why the enamel on the front side appears darker than that on the reverse side.

A composition similar to the above was found on the front side of the cross (Table 11: 1–3; Fig. 2: 1–3). The differences include a different compositional ratio (1.5), a lower cobalt content (0.26 %), and, in addition to manganese oxide (0.58 %), the presence of antimony oxide (0.63 %). The latter likely entered the glass along with the lead (Fig. 5a), indicating a different geochemical signature from the previous sample [5, P. 50]. Y.S. Freestone and K.P. Stapleton also report on antimony impurities in lead, referencing lead ore (galena) deposits near Kamsar (Iran, south of Kashan) that contain small amounts of antimony. These deposits were described by J.E. Dayton and J. Bowles [17, P. 126].

A completely different composition of deep-blue enamel was found on the reverse side of the temporal pendant (Table 10: 16; Fig. 1: 16). A soda-based enamel of the Na–Ca–Si chemical class was used, with limestone as the alkaline earth component. The components were combined at a ratio of 2. Cobalt oxide (0.23 %) was used as the colorant, antimony oxide (3.5 %) as the opacifier. The manganese oxide content (0.7 %) is sufficient to indicate its deliberate use as a decolorizer (Fig. 4b). However, V.A. Galibin strongly emphasized that manganese was not used as a decolorizer in soda glasses colored with cobalt. He argued that the presence of manganese in concentrations above 0.5 % (reaching up to 2 %) suggests the use of cobalt ores with manganese impurities (such as asbolane) or manganese ores with high cobalt content (wad). Such characteristics are typical of glass of "East Mediterranean European origin" as opposed to Eastern-type glasses, which used

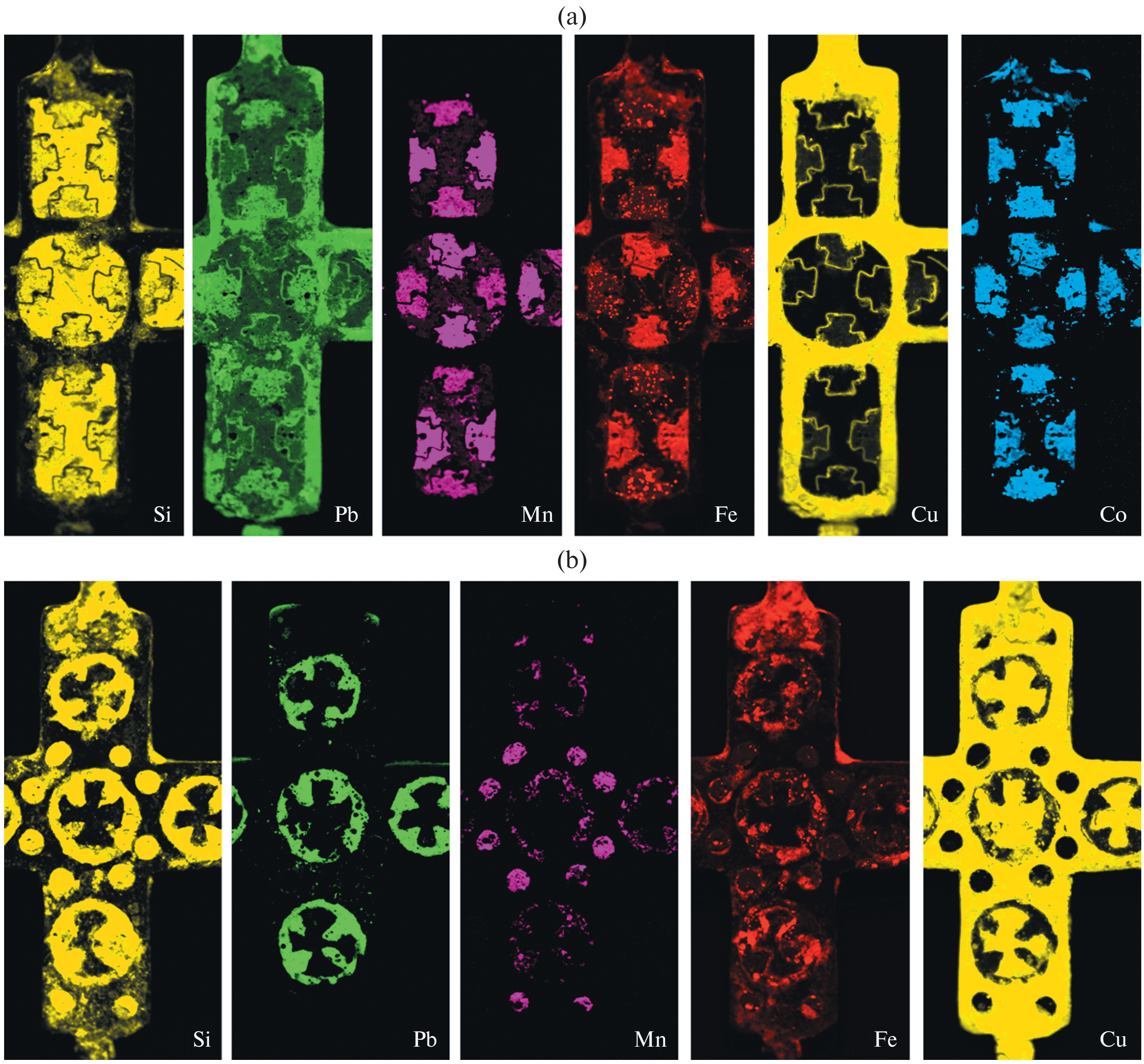

Fig. 5. Maps of the distribution of elements obtained by X-ray fluorescence mapping on the surface of the cross: a – front side, b – back side.

Iranian cobalt with negligible manganese impurities (above 0.3 %) [5, P. 37, 38]. We agree with his view, as none of the other soda enamels of different colors contain manganese.

A soda-based enamel was also used in one area of the front side of the temporal pendant (Table 9: 4; Fig. 1: 4). The high lead content (17.2 %) and low calcium content (4.29 %) allowed us to classify it chemically as Na–Pb–Si. Dolomitic limestones were used as the alkaline earth source. The compositional ratio, considering the lead concentration, was 1.25. The cobalt oxide content, which is the traditional colorant for deep-blue hues, is only 0.005 %, whereas in previous cases, its concentration was in the tenths of a percent. However, cobalt has a strong coloring effect and can tint glass even at a concentration of 0.001 % [5, P. 37]. The antimony oxide content (0.59 %) is likely indicative of its role as a decolorizer [18, P. 1226]. This suggests that, unlike all previous deep-blue enamels, this composition lacks an opacifier. However, attention should be given to the unusual appearance of this enamel, which fills a circular space formed by a gilded wire (Fig. 1: 4). The center features a deep-blue square, while the remaining areas appear gray. It is possible that the analysis was conducted at the boundary between these two colors, resulting in underestimated concentrations of certain elements and an overestimated lead content (Fig. 4a).

Red-brown enamel was used on both sides of the pendant-icon and on the front sides of the temporal pendant and the cross.

Table 7. Chemical composition of enamels on the front side of the pendant-icon

Color	Deep-blue		White	Red-brown			Grey	Black	Light grey	
Analysis area*	1	2	3	4	5	6	7	8	10	11
Class	Na–Ca–Si		Na–Ca–Si	Na–Ca–Si			Na–Ca–Si	Na–Ca–Si	Na–Ca–Si	
Source of alkalis	ash *Kalidium caspicum* annuals above-ground parts	ash *Kalidium caspicum* annuals above-ground parts	ash *Kalidium caspicum* annuals above-ground parts	ash *Kalidium caspicum* annuals above-ground parts	ash *Kalidium caspicum* annuals above-ground parts		soda	ash *Salicornia herbacea* annuals above-ground parts	ash *Kalidium caspicum* annuals above-ground parts	
Norm	1.25		*2*	1.5	*1.5*		2.5	*2*	1.5	
Lead	3 < Pb < 10		3 < Pb < 10						3 < Pb < 10	
Dye	Co *0.36–0.42*			Cu *1.24–1.32*			Mn *0.47*	Mn *3.5*		
Bleacher	Mn *0.57–0.62*		Mn *0.45*	Mn *0.91–1.49*					Mn *0.52*–0.59	
Muffler	Sn *4.93–5.08*		Sn *2.49*	Cu *1.24–1.32*			Sb *0.49* (?)		Sn 3.39–*3.73*	

Note: Results obtained using average values are shown in italics.
*The numbers of the analysis zones correspond to the numbers in Fig. 3.

Table 8. Chemical composition of enamels on the reverse side of the pendant-icon

Color	Deep-blue		Red-brown		Grey		Black
Analysis area*	12	13	14	15	16	17	18
Class	Na–Ca–Si		Na–Ca–Si		Na–Ca–Si		Na–Ca–Si
Source of alkalis	ash *Kalidium caspicum* annuals above-ground parts		ash *Kalidium caspicum* annuals above-ground parts	ash *Kalidium caspicum* annuals above-ground parts	soda		ash *Salicornia herbacea* annuals above-ground parts
Norm	1.25		1.5		2		*2*
Lead	3 < Pb < 10						
Dye	Co *0.36–0.44*		Cu *1.46–3.93*		Mn *0.45–0.51*		Mn *4.39*
Bleacher	Mn *0.61–0.69*		Mn *0.91–1.01*				
Muffler	Sn *4.56–5.08*		Cu *1.46–3.93*		Sb *0.39* (?)		

Note: Results obtained using average values are shown in italics.
*The numbers of the analysis zones correspond to the numbers in Fig. 3.

Table 9. Chemical composition of enamels on the front side of the temporal pendant

Color	Deep-blue				White	Turquoise		Red-brown					Grey
Analysis area*	1	2	3	4	5	6	7	8	9	10	11	12	13
Class	Na–Ca–Si			Na–Pb–Si	Na–Ca–Si	Na–Ca–Pb–Si		Na–Ca–Si				Na–Ca–Si	Na–Ca–Si
Source of alkalis	ash *Kalidium caspicum* annuals above-ground parts			soda	soda	ash *Kalidium caspicum* annuals above-ground parts		ash *Kalidium caspicum* annuals above-ground parts				soda	soda
Norm	1.25			1.25	1.75	*1.25*		1.5				1.5	2
Lead	3 < Pb < 10			Pb > 10		Pb > 10							
Dye	Co 0.38–0.62			Co 0.005		Cu 2.2–2.8		Cu 1.49–2.99				Cu 0.12 (?)	Mn 0.08 (?)
Bleacher	Mn 0.58–0.61					Mn *0.26* (?)		Mn 0.65–0.69					
Muffler	Sn *1.55*–1.62			Sb 0.59 (?)	Sb *4.23*	Sn 2.4–2.9		Cu 1.49–2.99				Cu 0.12 (?)	Sb 0.78 (?)

Note: Results obtained using average values are shown in italics.
*The numbers of the analysis zones correspond to the numbers in Fig. 1.

Table 10. Chemical composition of enamels on the reverse side of the temporal pendant

Color	Deep-blue	White	Turquoise	Yellow	
Analysis area*	16	17	18	19	20
Class	Na–Ca–Si	Na–Ca–Si	Na–Ca–Si	Na–Ca–Si	
Source of alkalis	soda	soda	soda	soda	
Norm	2	2.5	2.5	3	
Lead				3 < Pb < 10	
Dye	Co *0.23*		Cu *2.36*	Fe 0.45–1.13	
Bleacher					
Muffler	Sb *3.5*	Sb *2.02*	Sb *1.93*	Sb 0.53–0.81	

Note: Results obtained using average values are shown in italics.
*The numbers of the analysis zones correspond to the numbers in Fig. 1.

Table 11. Chemical composition of enamels on the front side of the cross

Color	Deep-blue			White			Red-brown		
Analysis area*	1	2	3	4	5	6	7	8	9
Class	Na_2O–CaO–SiO_2			Na_2O–CaO–SiO_2			Na_2O–CaO–SiO_2		
Source of alkalis	ash *Kalidium caspicum* annuals above-ground parts			soda			ash *Kalidium caspicum* annuals above-ground parts		
Norm	1.5			2			*1.5*		
Lead	3 < Pb < 10								
Dye	Co *0.26*						Cu *1.57*		
Bleacher	Mn *0.58*						Mn *0.95*		
Muffler	Sn *1.08*			Sb *4.04*			Cu *1.57*		

Note: Results obtained using average values are shown in italics.
*The numbers of the analysis zones correspond to the numbers in Fig. 2.

Table 12. Chemical composition of enamels on the reverse side of the cross

Color	White		Green	
Analysis area*	10	11	13	14
Class	$Na_2O–CaO–SiO_2$		$Na_2O–CaO–PbO–SiO_2$	
Source of alkalis	soda		soda	
Norm	*2*		*2*	
Lead			Pb > 10	
Dye			Cu *3.57*	
Bleacher				
Muffler	Sb *3.74*			

Note: Results obtained using average values are shown in italics.
*The numbers of the analysis zones correspond to the numbers in Fig. 2.

The enamels on both sides of the pendant-icon (Table 7: *4–6*; 8: *14*, *15*; Fig. 3: *4–6*, *14*, *15*) and some areas of the front side of the temporal pendant (Table 9: *8–11*; Fig. 1: *8–11*; 4a) turned out to be identical. This is Na–Ca–Si glass fused using the ash of plants from an arid zone (aboveground parts of the annual plant *Kalidium caspicum*) and dolomitic limestone. These two components were combined in a ratio of 1.5. The coloring agent and opacifier was metallic copper or cuprous oxide, while manganese oxide acted as a decolorizer. In all cases, a high content of iron oxide (from 3.33 to 5.25 %) was noted, added to facilitate copper reduction [19, P. 56].

The same enamel composition, except for an antimony impurity (0.19 %), was found on the front side of the cross (Table 11: *7–9*; Fig. 2: *7–9*; 5a). Here, this is probably also associated with lead, albeit in a small concentration (0.8 %), which entered the batch with the copper alloy.

A completely different composition of red-brown enamel is present in one of the areas on the front side of the temporal pendant (Table 9: *12*; Fig. 1: *12*; 4a). Here, Na–Ca–Si enamel was used, fused with soda and limestone in a ratio of 1.5. The copper content is extremely low (0.12 %), which is insufficient for coloration and opacification. Unlike the previous red-brown enamels, the iron oxide content is low (0.45 %), which is also unlikely to act as a colorant. However, antimony oxide was evidently used, with a concentration of 4.85 % indicating its use as an opacifier – something usually unnecessary in the production of opaque red-brown glass opacified with metallic copper or cuprous oxide. In this case, antimony was probably added to enhance the growth of copper particles [20, P. 117].

It is important to note that in all cases, the analysis of red-brown enamels showed a low lead concentration (0.04–3.88 %). A similarly low lead content characterizes Limoges enamels [19, P. 58]. This contrasts with the high lead concentration (15–30 %) typically found in so-called sealing-wax glass and Roman-era enamels.

White enamel was used on both sides of the temporal pendant and the cross, as well as on the front side of the pendant-icon.

The enamels on both sides of the temporal pendant (Table 9: *5*; 10: *17*; Fig. 1: *5*, *17*; 4) and the cross (Table 11: *4–6*; 12: *10, 11*; Fig. 2: *4–6, 10–12;* 5) turned out to be soda-based (Na–Ca–Si class) and opacified with antimony oxide. In the cross, dolomites were used as a source of alkaline earths, with the components combined in a ratio of 2. The same alkaline earth source was used for the enamel on the reverse side of the temporal pendant (Fig. 1: *17*), with a component ratio of 2.5. On the front side (Fig. 1: *5*), limestone was used, with a recipe ratio of 1.75.

A different composition was found in the white enamel on the front side of the pendant-icon (Table 7: *3*; Fig. 3: *3*). Here, Na–Ca–Si glass was used, fused with the ash of plants from an arid zone (*Kalidium caspicum*) and dolomitic limestone. These two components were combined in a ratio of 2. The composition includes a lead additive (4.69 %). In the absence of a colorant, tin was used as an opacifier. The manganese content (0.45 %) indicates its use as a decolorizer. The presence of antimony (0.99 %), as in the case of the deep-blue and red-brown enamels of the cross, is a geochemical characteristic of lead.

Gray enamel was identified on both sides of the pendant-icon (Table 7: *7*; 8: *16, 17*; Fig. 3: *7, 16, 17*) and on the front side of the temporal pendant (Table 9: *13*; Fig. 1: *13;* 4a). In all cases, Na–Ca–Si enamel was used, fused with soda and dolomitic limestone. However, different recipe norms (ratios) were applied: for the front side of the temporal pendant (Table 9: *13*; Fig. 1: *13*) and the reverse side of the pendant-icon, the ratio was 2 (Table 8: *16*, *17*; Fig. 3: *16, 17*), while for the front side of the pendant icon (Table 7: *7*; Fig. 3: *7*), it was 2.5. The antimony oxide content (0.39–0.78 %) suggests its use as a decolorizer, especially since the enamel here is not completely opaque. However, it is also not transparent but rather cloudy, translucent, and resembling stone, such as marble. Possibly, antimony in such a small concentration acted as a clouding agent, which was necessary in the production of enamel for depicting faces. A similar method for obtaining flesh-toned glass – introducing a reduced amount of antimony compared to the concentration needed for opaque white glass—has been noted in tesserae from Roman church mosaics [21, P. 18]. A small addition of manganese oxide (0.45–0.51 %) found in the pendant-icon enamel likely acted as a colorant, giving the glass a slightly pinkish hue, which was used for depicting faces [21, P. 13]. In the enamel of the temporal pendant, the manganese content is low (0.08 %) but relatively high (0.76 %) in areas deemed unsatisfactory in terms of the main components (sodium, potassium, calcium, magnesium, lead, and aluminum) and therefore excluded from the interpretation of results.

Green enamel is noted on the front side of the temporal pendant and the reverse side of the cross. The enamel on the reverse side of the cross (Table 12: *13, 14*; Fig. 2: *13, 14*; 5b) contains a high concentration of lead (11.69 %) and is therefore classified as Na–Ca–Pb–Si glass, fused with soda and limestone in a 2:1 ratio. Copper oxide (3.57 %) served as the colorant in the presence of lead. The composition also includes a tin impurity (0.9 %); however, the enamel remains transparent. Tin in this case is likely a byproduct of copper, which was introduced into the glass in the form of tin bronze. The ratio of tin to copper should not exceed 0.3 [5, P. 33]; in this case, it is 0.25.

The green enamel on the front side of the temporal pendant was possibly used to depict eyes (Table 1: *14*; Fig. 1: *14*; 4a). It has suffered severe degradation, making it impossible to determine the glass type, raw materials, or compositional ratios. However, it contains a significant amount of lead oxide (25 %) and copper oxide (4.4 %), which likely functioned as a colorant, suggesting that the depicted eyes were turquoise or green. Additionally, the enamel has a high iron oxide content (11.9 %).

Turquoise enamel is noted only on the temporal pendant, on both the front and reverse sides. Their compositions differ. On the front side of the temporal pendant (Table 9: *6, 7*; Fig. 1: *6, 7*; 4a), the enamel contains a high concentration of lead (16.9–18.43 %) and is classified as Na–Ca–Pb–Si glass, fused with plant ash from arid-zone vegetation (aerial parts of the annual plant *Kalidium caspicum*) and dolomite. These components were combined in a 1.25:1 ratio. The enamel was colored with copper oxide and opacified with tin oxide. The manganese content (0.26 %) is insufficient for decolorization. Interestingly, glass of similar composition, color, and transparency reappears in Rus during the Golden Horde period in the form of rings and beads [22, P. 245, 246; 23, P. 372].

For the turquoise enamel on the reverse side (Table 10: *18*; Fig. 1: *18*; 4b), Na–Ca–Si glass was used, fused with soda and dolomitic limestone in a 2.5:1 ratio. Copper oxide served as the colorant, and antimony oxide as the opacifier.

Yellow enamel is used only on the reverse side of the temporal pendant (Table 10: *19, 20*; Fig. 1: *19, 20*; 4b). The glass belongs to the Na–Ca–Si class, fused with soda and dolomitic limestone in a 3:1 ratio. Iron oxide (0.45–1.13 %) in the presence of lead (6.81–7.72 %) likely acted as the colorant [24, P. 228]. The antimony oxide concentration (0.58–0.81 %) is insufficient for opacification [11, P. 108], but since lead antimonate is traditionally considered the opacifier for opaque yellow glass [19, P. 54, 55], this concentration was likely adequate when using this compound.

Brown enamel, used only on the front side of the temporal pendant (Table 1: *15*; Fig. 1: *15*; 4a), is in poor condition. It has extremely low alkali and alkaline earth component content. A high concentration of lead oxide (31.5 %) was detected, along with copper (1.6 %), manganese (1 %), and iron (1.3 %).

Black enamel is present only on the pendant-icon, both on the front (Table 7: *8*; Fig. 3: *8*) and reverse side (Table 8: *18*; Fig. 3: *18*). In both cases, the glass is classified as Na–Ca–Si, fused with ash from the aerial parts of the annual plant *Salicornia herbacea*. Dolomitic limestone was used as the source of alkaline earths, with components combined in a 2:1 ratio. Manganese oxide, in high concentration (3.5–4.39 %), was used as the colorant.

Light gray enamel is noted only on the front side of the pendant-icon (Fig. 3: *9–11*). The glass can be classified as Na–Ca–Si with an increased lead content (6.25–8.19 %). Plant ash from arid-zone halophytes (*Kalidium caspicum*) was used as the alkali source, and dolomite as the alkaline earth source. Components were combined in a 1.5:1 ratio. Tin oxide (3.39–3.73 %) was used for opacification, while manganese oxide (0.52–0.59 %) was used for decolorization (Table 7: *10, 11*).

Thus, enamels of the same color exhibit different compositions. For example, deep-blue enamel appears in several types:

– ash-based, with high lead content, tin as an opacifier, manganese as a decolorizer, and compositional ratios of 1.25 and 1.5;

– soda-based, lead-free, with antimony as an opacifier;

– soda-based, with high lead content and antimony as an opacifier (?).

The first type, with a 1.25 ratio, is found on both sides of the pendant-icon and on the front side of the temporal pendant, while the 1.5 ratio is found on the cross. The second type is on the reverse side of the temporal pendant. The third type is in one zone of the temporal pendant's front side.

Red-brown enamel is identified in two types:

– ash-based, with copper as an opacifier and manganese as a decolorizer;

– soda-based, with antimony.

The first type is found on both sides of the pendant-icon, as well as the front sides of the temporal pendant and cross, while the second type appears in one zone of the temporal pendant's front side.

White enamel exists in two types:

– soda-based, with antimony as an opacifier;

– ash-based, with high lead content, tin as an opacifier, and manganese as a decolorizer.

The first type is noted on both sides of the temporal pendant and cross, but with different compositional ratios: 2 for the cross, 1.75 for the front side of the temporal pendant, and 2.5 for the reverse. The second type is present on the pendant-icon.

Turquoise enamel is found only on the temporal pendant, but in different types:

– on the front side: ash-based, with high lead content, opacified with tin oxide;

– on the reverse side: soda-based, lead-free, with antimony as an opacifier.

Other enamel colors belong to single types. Gray enamel is soda-based with antimony (?) as an opacifier. It appears on both the temporal pendant and pendant-icon but with different compositional ratios. Black enamel is ash-based, with manganese as the colorant. It is used only on the pendant-icon, on both sides. Yellow enamel is soda-based, with high lead content and antimony as an opacifier, found only on the reverse side of the temporal pendant. Light gray enamel is ash-based, with high lead content, opacified with tin, and decolorized with manganese, used only on the front side of the pendant-icon. Green enamel is soda-based, with high lead content, and is noted on the reverse side of the cross. A similar enamel may have been used for the front side of the temporal pendant, but it is in very poor condition.

Thus, both soda-based and ash-based enamels were used to decorate all three objects. Soda-based enamels contain antimony as an opacifier (except for transparent green enamel) and, in some cases, lead, which was used to color yellow and green enamels. In one instance, a high concentration of lead (over 10 %) was found in a deep-blue enamel.

Ash-based enamels (except for red-brown and black) contain tin as an opacifier, with lead concentrations below 10 %, except for turquoise enamel, which contains more than 10 %. Manganese was added to decolorize ash-based enamels (except black).

Six compositional standards for low-melting fractions were identified: 1.25, 1.5, 1.75, 2, 2.5, and 3. The 1.75, 2.5, and 3 standards were used exclusively with soda-based enamels, while the others were used for both soda- and ash-based glasses.

The greatest variety of enamel types was found on the temporal pendant, with 11 types (though the palette includes only eight colors), including three ash-based and eight (?) soda-based enamels. The pendant-icon features six enamel types, with only one soda-based and the rest ash-based. The cross has four enamel types, two of each kind.

On the pendant-icon, both ash- and soda-based enamels appear on both the front and back. On the temporal pendant and cross, all back-side enamels are soda-based, while both types are present on the front. Notably, different types of deep-blue and red-brown enamels were used on the front of the temporal pendant: ash-based enamels appear in several areas, while soda-based ones occur in only one area of the respective colors.

The highest matches between enamel types of the same color on the front and back were found on the pendant-icon, specifically for deep-blue, red-brown, black, and gray enamels, although the gray enamel differs in compositional standard. On the temporal pendant, only the white enamel is the same on both sides, though different compositional standards were used. On the cross, the white enamel is the only one that matches perfectly on both sides.

DISCUSSION

Interestingly, the enamels used to decorate the temporal pendant match compositions previously identified in Limoges enamels from the 10th–14th centuries [19]. Studies of these enamels revealed two groups: those made with soda and antimony, with lead content not exceeding 10 % (including in yellow and green enamels), and ash-based enamels where tin replaced antimony, with higher lead content. These two groups differ chronologically, with the second quarter of the 13th century marking the transition. Soda-based enamels belong to the earlier group, while ash-based enamels are later. However, during a short period at the end of the 12th–early 13th century, both types were used on the same objects [19, P. 55].

A similar pattern is observed in the present study. The backs of the temporal pendant and cross feature only early-group enamels, while their fronts include both early- and late-group enamels. The pendant-icon contains both groups on both sides.

This combination of two chronological enamel groups may suggest a dating of the objects to the late 12th–early 13th century. Moreover, the varying compositions of enamels of the same color on a single object suggest that the enameling was done by a jeweler unfamiliar with glassmaking, who received enamels in chunks or powdered form and selected them based on color alone.

The early-group soda-based enamels are closely related to the Roman glassmaking tradition, which, according to Limoges enamel researchers, may have persisted until the second quarter of the 13th century [19, P. 59]. While the exact location remains unclear, it is worth recalling that Roman glassmaking influenced the Byzantine glassmaking school, establishing a direct lineage from Roman to Byzantine traditions [15, P. 167; 16, P. 98]. This is supported by the compositional standards applied. Specifically, the 1.5, 1.75, 2, 2.5, and 3 standards have been known since antiquity and were used extensively in Roman glassmaking (~90 % of cases). The Byzantine school continued these traditions, though these standards became less dominant, comprising just over half of Byzantine glass compositions. The 1.25 standard is unique to the Byzantine school, where it accounted for slightly more than 15 % and, together with other exclusively Byzantine standards (0.75 and 1), made up about 40 % [16, P. 94, 95]. Notably, the Byzantine 1.25 standard appears not only in ash-based but also in soda-based enamels (in the deep-blue enamel on the front of the temporal pendant).

The idea that Roman glassmaking traditions persisted is tied to the use of soda as the alkali component. However, researchers highlight one major issue: it is generally believed that by the late 9th century, Near Eastern glassmakers had abandoned soda due to increased production demands and a shortage of Egyptian soda. Instead, they began using halophytic plant ash. The main reasons for the soda shortage were political, including internal instability in the Nile Delta and Wadi Natrun in the 7th–9th centuries, which disrupted soda production and exports from Egypt [25, P. 194; 26, P. 528–529]. Consequently, by the 11th century, soda-based glass production in the Near East had nearly ceased, and glassmakers switched to halophytic ash, a traditional raw material in Mesopotamia and Syria since the Bronze Age.

Furthermore, it is believed that the use of antimony ceased no later than the mid-4th century [18, P. 1234]. However, this claim is contradicted by research showing antimony's presence in white enamel from the 9th-century altar of Saint Ambrose in Milan, which was made with plant ash. Additionally, in the soda-based glass mosaics of Roman churches, antimony was used continuously from the 4th to the 12th century. Only in the 13th century did Roman mosaic tesserae production transition to tin-based opacifiers [21, P. 18]. However, evidence suggests that antimony continued to be used as an opacifier even later. For example, an Italian (Castelli, Abruzzo) majolica vessel from the 16th century in the Nizhny Novgorod State Art Museum contains 3 % antimony in its white, opaque, lead-based (alkali-free) glaze [27, P. 117, Table 1]. A similar composition (lead-silica glass with 1.8 % antimony) was found in a black glass bead from the Nastasino settlement near Moscow, dated to the 13th–15th centuries [28, P. 69–70].

In addition to the soda-based enamels of the objects under consideration and the aforementioned enamels of Limoges, as well as the enamels of the Byzantine golden encolpion from the mid-10th century [19, P. 59] and certain enamels from the golden quadrifoliate pendant from Novgorod dating to the early 13th century [29, P. 113–114], also produced with soda, a number of artifacts made from soda glass are known, dating to the early–first third of the 2nd millennium AD. Among them are bracelets made of blue, purple, and green glass from the 10th–12th centuries found in the Byzantine fortress of Isaccea (Vicina) in Romania [30, P. 1026, 1029], as well as bracelets of white, purple, and green glass from the 11th–12th centuries discovered in the Byzantine urban center located in the present-day village of Nufăru (Preslavitza) in Romania [31, P. 2882, 2887]. In addition to the aforementioned mosaic glasses from churches in Rome dating from the 4th to 12th centuries, there is evidence of soda glass from the 9th–13th centuries found in other parts of Italy [32, P. 83]. Similar finds have also been discovered in Rus': a deep-blue bead from a late 12th-century burial within the Dmitrov Kremlin in the Moscow region [33, P. 126, 132, Table]; a black ring adorned with multicolored glass fragments from the Dmitrov Kremlin [22, P. 248, Table 2, An. No. 754–48; 23, P. 369, Table 2, No. An. 754–48]; rings made of opaque turquoise glass from the Moscow Kremlin, one of which is dated to the second half–end of the 13th century [34, P. 222, 305, 310, Tables II, III; 22, P. 247, Table 2, An. No. 725–24, 32; 23, P. 367, Table 2, No. An. 725–24, 32]; a deep-blue vessel from the 10th–13th centuries from Novgorod and smalt of the same color from the 11th–13th centuries found in St. Sophia Cathedral in Kyiv [5, P. 37, Table 15, 1850, 1912]; a fragment of a colorless glass vessel with enamel and gold decoration from the first half of the 14th century discovered in Pereyaslavl Ryazansky [35, P. 333]; and a fragment of a vessel from Tver dating to the late 14th century [36, P. 143].

Researchers propose two possible explanations for the continued existence of soda-based glass beyond the 11th century. The first hypothesis, based on Theophilus's account, suggests that glass from Roman mosaics, particularly in Italy, was repurposed for enamel work. This explanation was specifically proposed for the soda-based enamels of the golden quadrifoliate pendant from Novgorod dating to the early 13th century [29, P. 116]. However, scholars of Limoges enamels note that it is difficult to believe that a sufficient quantity of Roman mosaics was available to sustain enamel production in Limoges and the Meuse Valley for several centuries. Moreover, the consistency in the composition of different colored Limoges enamels does not align well with the idea of an unstable supply of Roman tesserae over several centuries [19, P. 58].

The second hypothesis, which we support, suggests the existence of alternative sources of soda or other natural sources of sodium beyond Wadi Natrun in Egypt [19, P. 59]. Several saline lakes are known today that could have served as such sources [37, P. 126], such as Lake Pikrolimni in Greek Macedonia, described by Pliny. An analysis of water from this lake, considered a sodium source in Roman and early Byzantine times, confirmed an elevated concentration of sodium bicarbonate [38]. Since the Roman period, Lake Van in eastern Anatolia has been an important source of soda, as mentioned by Strabo and the 12th-century metropolitan of Thessaloniki, Eustathius. These historical accounts were substantiated by an analysis of water samples from the lake, revealing carbonate concentrations approximately 100 times higher than in seawater. Another potential soda source is Lake Al-Jabbul in northern Syria, southeast of Aleppo. Documentary evidence also points to a soda source at Lake Tarabiya in Upper Egypt, which was first exploited in the 9th century [26, P. 523–524; 39, P. 66–67]. Furthermore, written sources indicate that soda extraction was resumed around 1190 at Wadi Natrun in Egypt [26, P. 528]. Although the sources do not specify the intended use of the extracted soda, it can be assumed that it was employed in glassmaking.

The near-identical chemical composition of the enamels of the examined objects and those of Limoges suggests that the glass used for enamels was not locally produced but originated from a single production center, presumably in Byzantium. For instance, according to T. I. Makarova, the Byzantines were the inventors of a green transparent enamel resembling an emerald [4, P. 4], which may be present on the reverse side of the cross under study. It is likely that Byzantium had a specialized enamel glass production industry (as indicated by certain characteristics of some enamels, such as the opacification of deep-blue enamels, a feature never observed in other glass objects of this color). This industry, up until the early 13th century, continued Roman glassmaking traditions based on soda glass. After this period, a shift occurred, marking a transition to potash-based glass for enamel production. This turning point may be linked to historical events in Byzantium at the time—specifically, the capture of Constantinople by the Crusaders in 1204.

CONCLUSION

Regarding the place of manufacture of the examined objects, it is possible that they were produced in Kyiv. This is indirectly supported by the near-identical composition of the studied enamels and those from Limoges. It is evident that Kyiv, like Limoges, obtained its enamels directly from Byzantium. Their further distribution across Rus' would likely have resulted in compositional mixing (through the addition of locally produced enamels). Another perspective on their origin is based on T. I. Makarova's view that enamel artisans were relocated from Kyiv to Vladimir by Andrey Bogolyubsky. Makarova arrived at this conclusion by linking the golden temporal pendants from the Vladimir hoards to Kyiv traditions [4, P. 34, 35, 99]. This hypothesis is indirectly supported by the find locations of the examined objects. It is worth noting that T. F. Mukhina, in her initial description of the temporal pendant, also leaned toward attributing it to Vladimir [6, P. 154]. In any case, whether the artisans were of Rus' origin or foreigners (the latter hypothesis has been suggested, for instance, for an pendant-icon [9, P. 211]), they must have maintained close ties with Kyiv.

FUNDING

The work was carried out within the state assignment of the National Research Centre "Kurchatov Institute" using the equipment of the Shared Research Center "Structure diagnostics of materials" in the part of XRF studies.

CONFLICT OF INTERESTS

The authors have no conflicts of interest.

REFERENCES

1. *Kondakov N.P.* History and monuments of Byzantine enamel. St. Petersburg: M.M. Stasyulevich printing house, 1892. 394 p.
2. *Zabelin I.E.* Historical review of enamel and price making in Russia. St. Petersburg: type. Expedition for procurement of state papers, 1853. 394 p.
3. *Drozdov A.A., Andreev M.N.* // History and pedagogy of natural science. 2018. No. 4. P. 49.
4. *Makarova T.I.* Cloisonne enamels of Ancient Rus'. Moscow: Nauka, 1975. 133 p.
5. *Galibin V.A.* Glass composition as an archaeological source. Ars vitraria experimentalis. (Proceedings of the IIMC RAS. Vol. 4). St. Petersburg: Petersburg Oriental Studies, 2001. P. 216.
6. *Mukhina T.F.* // Archaeology of the Vladimir-Suzdal land. Proceedings of the scientific seminar. Issue 2. Moscow: Institute of Archaeology of the Russian Academy of Sciences, 2008. P. 147.
7. *Stolyarova E.K., Zaitseva I.E., Mukhina T.F. et al.* // Interdisciplinary studies of cultural heritage sites using natural science methods: Proceedings of the All-Russian Scientific Conference (Simferopol, October 5–7, 2022) / Ed. Khairedinova E.A., Yatsishina E.B. Simferopol: Antikva, 2022. P. 143.
8. *Makarov N.A., Zaitseva I.E.* // Russian archeology. 2019. No. 4. P. 182.
9. *Stolyarova E.K., Kovalenko E.S., Murashev M.M. et al.* // Medieval arts and crafts. On the 90th anniversary of the birth of Tatyana Ivanovna Makarova. Moscow: Institute of Archaeology of the Russian Academy of Sciences, 2021. 185 p.
10. *Kovalenko E.S., Murashev M.M., Stolyarova E.K. et al.* // Crystallography Reports. 2020. V. 65. No. 6. P. 1073.
11. *Shchapova Yu.L.* Ancient glass. Morphology, technology, chemical composition. M.: MSU, 1989. 120 p.
12. *Ščapova J.* // Research on Glass of the Lusatian and Pomeranian Cultures in Poland / Ed. Malinowski T. (Archaeologia interregionalis. V. 12). Słupsk: Academia Paedagogica, 1990. 87 p.
13. *Stawiarska T.* Szkła z okresu wpływów rzymskich z Północnej Polski. Studium technologiczne. Wrocław; Warszawa; Kraków; Gdańsk; Lódz: Ossolineum, 1984. 156 p.
14. *Stolyarova E.K.* // Proceedings of the II (XVIII) All-Russian Archaeological Congress in Suzdal. Vol. 3. Moscow: Institute of Archaeology of the Russian Academy of Sciences, 2008. P. 405.
15. *Shchapova Yu.L.* Essays on the history of ancient glassmaking (based on materials from the Nile Valley, the Middle East and Europe). Moscow: Moscow State University, 1983. 200 p.
16. *Shchapova Yu.L.* Byzantine glass. Essays on history. Moscow: Editorial URSS, 1998. 288 p.

17. *Freestone I.C., Stapleton C.P.* // Gilded and enamel glass from the Middle East / Ed. Ward R. London: British Museum, 1998. 122 p.
18. *Schibille N., Sterrett-Krause A., Freestone I.C.* // Archaeol. Anthropol. Sci. 2017. V. 9. No. 6. P. 1223.
19. *Biron I., Dandridge P., Wypyski M.T. et al.* // Enamels of Limoges 1100–1350. New York: The Metropolitan Museum of Art, 1996. 48 p.
20. *Barber D.J., Freestone I.C., Moulding K.M.* // From Mine to Microscope. Advances in the Study of Ancient Technology / Eds. Shortland A.J. et al. Oxford: Oxbow Books, 2009. 115 p.
21. *Verità M., Santopadre P.* // J. Glass Studies. 2010. V. 52. P. 11.
22. *Stolyarova E.K.* // Krajinou archeologie, krajinou skla. Studie věnované PhDr. Evě Černé (Through the Landscape of Archaeology, Landscape of Glass. Studies dedicated to PhDr. Eva Černá) / Eds. Tomková K., Venclová N. Praha: Archeologický ústav AV ČR, Praha; Most: Ústav archeologické památkové péče severozápadních Čech, 2020. 241 p.
23. *Stolyarova E.K.* // The Age of Horsemen in the North Caucasus: on the 90th Anniversary of Vera Borisovna Kovalevskaya. Ed. by Albegova Z.Kh. et al. Moscow: Institute of Archaeology of the Russian Academy of Sciences, 2021. 362 p.
24. *Drozdov A.A., Andreev M.N.* // A Lifelong Search: On the 90th Anniversary of Yulia Leonidovna Shchapova. Moscow: INFRA-M, 2022. 226 p.
25. *Whitehouse D.* // J. Glass Studies. 2002. V. 44. P. 193.
26. 26. *Shortland A., Schachner L., Freestone I. et al.* // J. Archaeol. Sci. 2006. V. 33. P. 521.
27. 27. *Medvedeva S.V.* Research and restoration of the Italian majolica vessel of the 16th century from the Nizhny Novgorod State Art Museum. Diploma work. 2009. M. 137 p.
28. *Stolyarova E.K.* // Medieval settlement Nastasino. (Works of the Moscow Region Expedition of the Institute of Archaeology of the Russian Academy of Sciences. Vol. 2). Moscow: Institute of Archaeology of the Russian Academy of Sciences, 2004. 69 p.
29. *Valiulina S.I., Rumyantseva O.S., Vaschenkova E.S. et al.* // Russian Archeology. 2022. No. 3. P. 107.
30. *Bugoi R., Poll I., Mănucu-Adameşteanu Gh. et al.* // J. Radioanal. Nucl. Chem. 2016. V. 307. No. 2. P. 1021.
31. *Bugoi R., Poll I., Mănucu-Adameşteanu Gh. et al.* // J. Archaeol. Sci. 2013. V. 40. P. 2881.
32. *Verità M., Zecchin S.* // Produzione e distribuzione del vetro nella storia: un fenomeno di globalizzazione. Atti delle XI Giornate Nazionali di Studio sul vetro in memoria di Gioia Meconcelli (Bologna, 16–18 dicembre 2005). Trieste: Editreg, 2011. P. 81.
33. *Stolyarova E.K.* // Antiquities of the Poochya. Collection of scientific works for the 60th anniversary of V.V. Sudakova. ComP. Gomzin A.A., Zavyalov V.I., Kusova I.G.; resP. ed. Nikitin A.O. Ryazan: RICO, 2016. 124 p.
34. *Stolyarova E.K.* Glass of medieval Moscow: 12th–14th centuries. Moscow: RSUH, 2016. 692 p.
35. *Stolyarova E.K.* // Complex archaeological research of Pereyaslavl Ryazansky. Responsible. editor and compiler. Zavyalov V.I. (Materials on the archeology of Pereyaslavl Ryazansky. Issue 3). Moscow: Taus, 2019. 319 p.
36. *Egorkov A.N.* // Tver Kremlin. Comprehensive archaeological source studies (based on the excavation materials of Tver Kremlin-11, 1993–1997). St. Petersburg: European House, 2001. 138 p.
37. *Nenna M.-D.* // Facta. 2007. V. 1. P. 125.
38. *Ignatiadou D., Dotsika E., Kouras A. et al.* // Annales du 16e Congrès de AIHV. Nottingham: AIHV, 2005. 64 p.
39. *Phelps M., Freestone I.C., Gorin-Rosen Y. et al.* // J. Archaeological Science. 2016. V. 75. P. 57.